Variety Management in Manufacturing. Proceedings of the 47th CIRP Conference on Manufacturing Systems

Analysis of the Process Dynamics for the Precision Honing of Bores

Christina Schmitt[a],*, Dirk Bähre[a]

[a]*Institute of Production Engineering, Saarland University, 66123 Saarbrücken, Germany*

* Corresponding author. Tel.:+49-681-30257559; fax: +49-681-3024858. *E-mail address:* Christina.schmitt@mx.uni-saarland.de

Abstract

The finishing of precise bores is an important machining step, especially in the automotive industries. Bores can vary in diameter and form, from bigger piston bores in motor cylinders to rather small bores in fuel injection systems. Quality parameters for these bores are form- and geometric accuracy as well as surface roughness and structure. All requirements can economically be met by using the honing process as the final finishing operation for readymade bores. Honing is an abrasive machining process using abrasive grains usually made of diamond or Cubic Boron Nitride (CBN) in metallic bonding. During the process three movement components, namely an axial movement along the bore axis, a rotational movement around the bore axis and the feeding movement of the honing stone, are combined. The feeding movement of the honing stone is induced by an axial movement of the feeding cone, which is translated into a radial movement of the honing stone at the interface between honing stone and work piece. The feeding movement is decisive for the results of the honing process. For a regulation of the process that enables high process stability and repeatability as well as good quality results from the first part it is important to know about the forces in the feeding system of the tool. The following paper describes the static and dynamic correlation of the process forces in order to give a basis for a new regulation approach especially for bores with smaller diameters (below 20mm) where the direct measurement of the process forces with a tool-integrated sensor is difficult. Measured signals are investigated for their dynamic influences. The theoretical approach is then compared to signals measured during the process.

1. Introduction

The honing process is often used where high requirements regarding geometric and form accuracy as well as surface quality are given [1, 2, 3]. This is often the case in the automotive industry. While long stroke honing can be used for a large range of different work piece dimensions and materials, the focus here is on the honing of small diameters up to 20mm in hardened steel. Decisive for the results of the honing process is the regulation method used. The classic feed controlled approach shifts the honing stone outwards in certain steps (Feed per time interval Z) within certain time intervals (P). When the planned material removal is reached, the process ends. Occurrences during the process, e.g. strongly raising forces are not regarded. However, the feed controlled approach can generate very good results, if the parameters are set correctly and fit to the process. But, as there are no given parameters for new processes, every process needs a running-in period to find the fitting parameters. For a serial production feed controlled honing is a good approach, but the rather long

running-in periods are a problem for productions with higher variety and thus smaller lot sizes. A newer approach called force controlled honing can help in this case [4] and enable a more flexible production which is getting more and more important [5]. It measures the process forces and tries to keep them constant by an adapted feeding of the honing stone. Force controlled honing is supposed to generate better quality results because of the constant forces and to remove the long running-in periods needed for feed controlled honing. The problem for force controlled honing, especially when smaller diameters are concerned, is the indirect measurement of the process forces above the feeding unit. This leads to a force signal that contains disturbances, especially friction forces and compliances. To enable a good regulation the disturbances have to be known and compensated. A theoretical approach is shown in the following; a signal calculated with this approach will furthermore be compared to a signal measured during the process.

Nomenclature

F_k Force at the feeding cone
F_{hr} Radial force at the honing stone
F_{ha} Axial force at the honing stone
M Moment around the tool

2. The honing process

Figure 1 shows the basic principle of the honing process using a single stone honing tool. There are three movement components combined. These are a rotational movement around the tool axis, an oscillating movement along the tool axis and the radial feeding movement of the honing stone. The feeding movement of the honing stone has an important influence on the process results and can be executed in different ways, as described above.
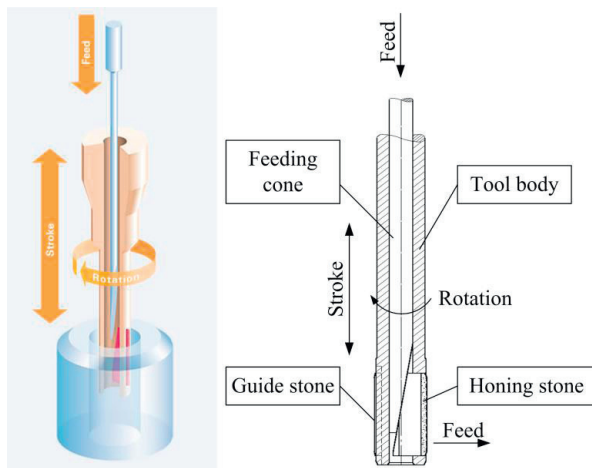

Fig. 1.Long-stroke honing [1].

The long stroke honing of bores with a diameter below 20mm is usually done by single stone tools equipped with one honing stone and two guiding stones which should not participate in the abrasive action, but guide the tool in the bore.
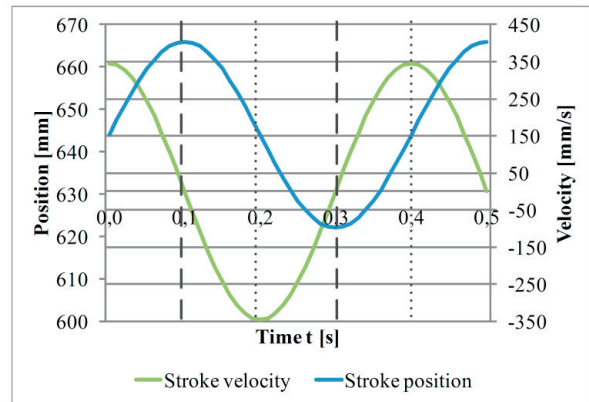

Fig. 2. Stroke position and velocity during the honing process.

Figure 2 takes a closer look at the stroke movement, which has a huge influence on the measured forces. During the upwards movement of the tool, the stroke velocity has positive values, during the downward movement it has negative values.

Theoretical approaches have been made by several authors, including Zettel, who considered forces during the honing process for a four-stone tool with a hydraulic feeding system [6] and Mushardt [7].

3. Theoretical process model
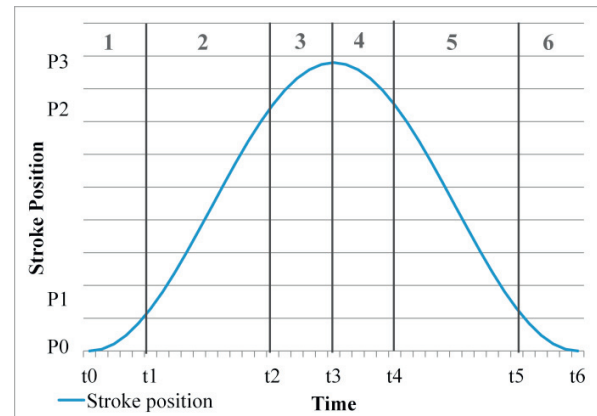
3.1. Process phases

Fig. 3. Phases of the Honing process.

Figure 3 shows the different phases of the stroke movement with the corresponding times and positions. Phase 1 represents the beginning of the upward movement in the lower reverse movement of the honing tool. The tool starts at

the lowest position, the lower reverse stop P0. Phase 2 begins at the position P1 and describes the continuous upward movement until the upper reverse movement starts by slowing down the tool. Phase 3 relates to the beginning of the upper reverse movement up to the upper reverse stop. Phase 4 describes the beginning of the downward movement coming from the upper reverse stop, the highest position P3. The tool is accelerating until the beginning of Phase 5. Phase 5 is the downward stroke movement and Phase 6 the slowing down until the lower reverse stop P0 is reached. After that the stroke movement begins anew with Phase 1. In a theoretical model all 6 phases have to be dealt with separately because of the different inertia effects.

3.2. Forces at the tool during the continuous phases

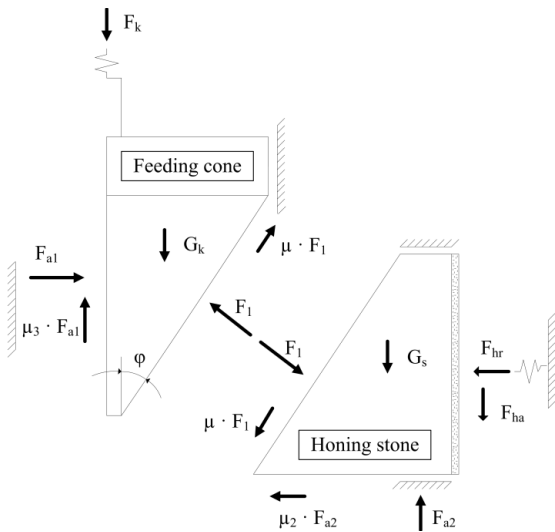

Fig. 4.Forces at the tool during the upward movement (Phase 2).

Figure 4 shows the force relations at the honing tool for the upward movement (Phase 2), which is described as a continuous movement. F_k is the force at the feeding cone. As the coefficients of friction μ between feeding cone and honing stone, μ_2 between honing stone and tool, and μ_3 between feeding cone all relate to a friction steel on steel they can be assumed to have the same value μ. Using the balance of forces at feeding cone (1: vertical, 2: horizontal) and honing stone (3: vertical, 4: horizontal), gives the following formulas (1) to (4):

$$-F_k + \mu \cdot F_{a1} + \mu \cdot F_1 \cdot \cos(\varphi) + F_1 \cdot \sin(\varphi) - m_k \cdot g = 0 \quad (1)$$

$$F_{a1} - F_1 \cdot \cos(\varphi) + \mu \cdot F_1 \cdot \sin(\varphi) = 0 \quad (2)$$

$$F_{a1} - F_{ha} - \mu \cdot F_1 \cdot \sin(\varphi) - F_1 \cdot \cos(\varphi) - m_l \cdot g = 0 \quad (3)$$

$$-F_{hr} - \mu \cdot F_{a2} - \mu \cdot F_1 \cdot \cos(\varphi) + F_1 \cdot \cos(\varphi) = 0 \quad (4)$$

F_{hr} can then be evaluated as depicted in Formula (5) using the friction coefficient μ and the cone angle φ.

$$F_{hr} = -\frac{1}{2 \cdot \mu \cdot \cos(\varphi) - \mu^2 \cdot \sin(\varphi) + \sin(\varphi)} \cdot (\mu^2 \cdot \sin(\varphi) \cdot (F_k + m_k \cdot$$

$g + 2 \cdot \square 2 \cdot cos\varphi \cdot Fha - \square 3 \cdot sin\varphi \cdot Fha + \square sin\varphi \cdot Fha + 2 \cdot ml \cdot g \cdot \square 2 \cdot c$
$os\varphi - ml \cdot g \cdot \square 3 \cdot sin\varphi + ml \cdot g \cdot \square sin\varphi + \square cos\varphi \cdot Fk + mk \cdot g + \square sin$
$\varphi \cdot Fk + mk \cdot g - cos\varphi \cdot Fk + mk \cdot g)$

$$(5)$$

The radial force on the honing stone F_{hr} in Formula (5) is only dependent on the values for μ, φ, the weight of the feeding unit m_k and the honing stone m_l and the signals for F_k and F_{ha}, which can be measured during the process.

The next step describes the downward movement in Phase 5, which is also a continuous movement. The balance of forces is therefore very similar, the difference is the axial force, which changes its direction as well as the bearing force between honing stone and tool body F_{a2}. F_{hr} in this case is:

$$F_{hr} = -\frac{1}{2 \cdot \mu \cdot \cos(\varphi) - \mu^2 \cdot \sin(\varphi) + \sin(\varphi)} \cdot (\mu^2 \cdot \sin(\varphi) \cdot (F_k + m_k \cdot$$

$g + 2 \cdot \square 2 \cdot cos\varphi \cdot Fha - \square 3 \cdot sin\varphi \cdot Fha + \square sin\varphi \cdot Fha + 2 \cdot ml \cdot g \cdot \square 2 \cdot c$
$os\varphi - ml \cdot g \cdot \square 3 \cdot sin\varphi + ml \cdot g \cdot \square sin\varphi + 2 \cdot \square cos\varphi \cdot Fk + mk \cdot g - cos$
$\varphi \cdot Fk - mk \cdot g) \qquad (6)$

3.3 Forces during the reverse movement

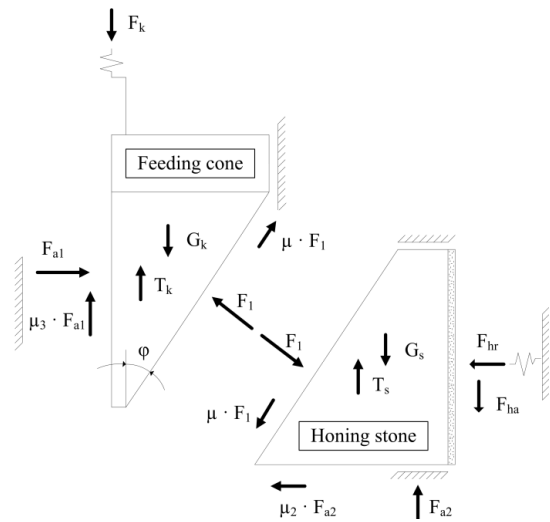At Phase 3, the beginning of the upper reverse movement, the force relations are depicted in figure 5.

Fig. 5.Forces at the tool during the upper reverse movement.

In this phase, the tool is slowing down as it approaches the upper reverse stop. In this phase the forces as described in 3.2 for the upwards movement have to be complemented by the inertia forces for feeding unit T_k and honing stone T_s, which are in an upwards direction as feeding unit and honing stone are set against the slowed movement. With the introduction of

these inertia forces, the force balance in Phase 3 gives with the acceleration zpp of the tool:

$$-F_k + \mu \cdot F_{a1} + \mu \cdot F_1 \cdot \cos(\varphi) + F_1 \cdot \sin(\varphi) - m_k \cdot g \\ + m_k \cdot zpp = 0 \qquad (7)$$

$$F_{a1} - F_1 \cdot \cos(\varphi) + \mu \cdot F_1 \cdot \sin(\varphi) = 0 \qquad (8)$$

$$F_{a1} - F_{ha} - \mu \cdot F_1 \cdot \sin(\varphi) - F_1 \cdot \cos(\varphi) - m_l \cdot g + m_l \cdot zpp = 0 \\ (9)$$

$$-F_{hr} - \mu \cdot F_{a2} - \mu \cdot F_1 \cdot \cos(\varphi) + F_1 \cdot \cos(\varphi) = 0 \qquad (10)$$

From these formulas (7) to (10) the radial force F_{hr} can again be deducted as before:

$$F_{hr} = -\frac{1}{2 \cdot \mu \cdot \cos(\varphi) - \mu^2 \cdot \sin(\varphi) + \sin(\varphi)} \cdot (\mu^2 \cdot \sin(\varphi) \cdot (F_k + m_k \cdot$$
$g - \square 2 \cdot \sin\varphi \cdot mk \cdot zpp + 2 \cdot \square 2 \cdot \cos\varphi \cdot Fha - \square 3 \cdot \sin\varphi \cdot Fha + \square \sin\varphi$
$\cdot Fha + 2 \cdot ml \cdot g \cdot \square 2 \cdot \cos\varphi - ml \cdot g \cdot \square 3 \cdot \sin\varphi + ml \cdot g \cdot \square \sin\varphi + \square \cos$
$\varphi \cdot Fk + mk \cdot g - \square \cos\varphi \cdot mk \cdot zpp - 2 \cdot ml \cdot zpp \cdot \square 2 \cdot \cos\varphi + ml \cdot zpp \cdot$
$\square 3 \cdot \sin\varphi - ml \cdot zpp \cdot \square \sin\varphi + \cos\varphi - \square \sin\varphi \cdot mk \cdot zpp + \square \sin\varphi \cdot Fk$
$+ mk \cdot g - \cos\varphi \cdot Fk + mk \cdot g)$

$$(11)$$

The same can be done for the reverse phase 1, 4 and 6 to get formulas for these sections as well. For phases 1 and 4 the formulas of the upward movement have to be used as the basis, and be complemented by the inertia forces in different directions. Phase 6 has as a basis the downward movement as well as phase 3, but the inertia forces are directed downwards in this case.

3.3. Moment around the tool

The forces around the circumference of the honing tool are shown in figure 6. The moment around the tool can be calculated using the correlation

$$M = r_w \cdot (F_{ht} + F_{s1t} + F_{s2t}) \qquad (12)$$

The tangential force components in formula (12) F_{ht}, F_{s1t} and F_{s2t} are in a certain relation to the radial force components F_{hr}, F_{s1r} and F_{s2r}. F_{hr} can be calculated as a function of the cone force F_k and the axial force F_{ha} as shown in the chapters 3.2 and 3.3 using the tool geometry for the different process phases (ε: angle between honing stone and guiding stone, δ: angle between the two guide stones, and cone angle φ between feeding cone and honing stone as shown in Figure 4). As previous studies show, there is a proportional relation between F_{ht} and F_{hr} [8, 9].

The ratio between tangential and normal force at the honing stone has been defined by [8] as the tangential force ratio μ_h:

$$\mu_h = \frac{F_t}{F_n} = \frac{F_{ht}}{F_{hr}} \qquad (13)$$

With the help of the tangential force ratio, the relation between the normal and tangential forces at the honing stone can be calculated. This gives:

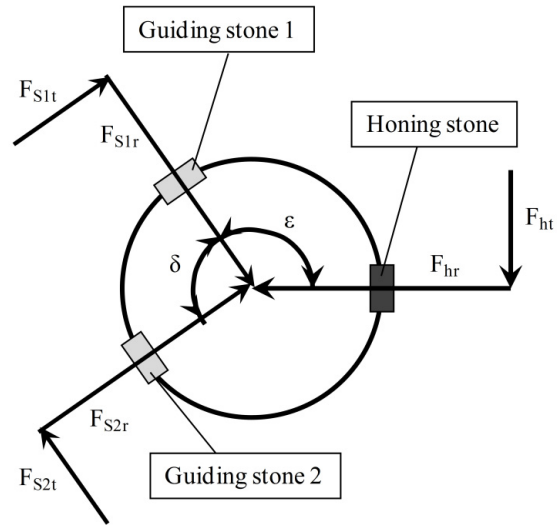$$F_{ht} = \mu_h \cdot F_{hr} \quad \text{with } F_{hr} = f(F_k, \text{tool geometry}) \qquad (14)$$

Fig. 6. Forces around the honing tool.

The same can be supposed for the guiding stones.

$$F_{s1t} = \mu_{s1} \cdot F_{s1r} \quad \text{and} \quad F_{s2t} = \mu_{s2} \cdot F_{s2r} \qquad (15)$$

If two identical guide stones are used, as it is usually done, it can be assumed that $\mu_{s1} = \mu_{s2} = \mu_s$. This gives the moment as:

$$M1 = r_w \cdot (\mu_h \cdot F_{hr} + \mu_s \cdot F_{s1r} + \mu_s \cdot F_{s2r}) \qquad (16)$$

F_{s1r} and F_{s2r} can be evaluated using the power balance at the honing tool as shown in Figure 6 with the assumption of a gimbal mounted work piece (no lateral forces).

$$F_{s1r} = \mu_s \cdot F_{s2r} + F_{hr} \cdot \sin(\varepsilon - \delta) - \mu_h \cdot F_{hr} \cdot \cos(\varepsilon - \delta) \qquad (17)$$

$$F_{s2r} = \frac{(F_{hr} \ast ((\mu_h - \mu_s) \ast \sin(\varepsilon - \delta) + (\mu_s \ast \mu_h + 1) \ast \cos(\varepsilon - \delta)))}{(\mu_s^2 + 1)} \qquad (18)$$

For the different phases different formulas for the moment can be deducted, which all follow the same structure:

$$M = a \cdot F_k + b \cdot F_{ha} + c \qquad (19)$$

with different coefficients a, b and c for the different phases. These coefficients are dependent on μ_s, μ_h, μ, φ, ε and δ. All those are known for a certain honing process.

4. Experimental setup

The experiments have been conducted on a single-spindle vertical honing machine by the Kadia Produktion+Co Gmbh, Nürtingen, Germany. The work pieces are made from

hardened steel, with a bore diameter of 7.98mm and an outer diameter of 25mm. The resulting wall thickness of around 8.5mm shall ensure that there is no influence from deformation of the work piece. For the experiments a single-stone tool is used. The abrasive grains of the honing stone are made from CBN and have a grit size of 90µm. The grains are embedded in a metallic sintered bonding. The stroke position of the Honing tool as well as the cone force have been recorded during the process using machine data. In addition an external force measuring device was used to record the axial force beneath the work piece and the moment at the work piece. The parameters used during the experiments are shown below in Table 1. The tangential force coefficient for the combination honing stone, workpiece material and honing oil has been determined in earlier experiments as μ_h=0.192 [9]. The tangential force coefficient for the guiding stone has been determined in the same way as μ_s=0.17 [9]. The cone angle φ of the used single-stone tool is 2.5°, the angle between honing and feeding stone ε is 125° and the angle δ between the guiding stones is 90° for the used tool. The weight of the feeding unit m_k is 0.5kg, the weight of the honing stone m_l is 0.002kg.

Table 1. Experiment parameters.

Parameter	Value	Unit
Honed diameter	0.008	m
Stroke velocity	2.6	m/s
Stroke acceleration	5	m/s2
Stroke length	44	mm
Rotation speed	1600	Min^{-1}
Radial feed per step	0.0005	Mm
Time between feed steps	0.25	S
Relaxation Time	2	s
Workpiece material	20MnCr5	
Honing stone	CBN grains	

The stroke length was 44mm. Each honing process includes several stroke movements. Figure 7 shows the stroke position for one oscillation and the measured signals cone force F_k and axial force F_{ha}. The time needed for one whole oscillation is 0.47s. The time and positions at the end of the different phases are for the given parameters:

1) Beginning of the upward movement of the tool
   T1 = 0.05s; H1 = 6.8mm
2) Upward movement
   T2= 0.17s; H2=37.2mm
3) Beginning of the upper reverse movement of the tool
   T3=0.22s; H3 = 44mm
4) Beginning of the downward movement
   T4=0.27s; H2=37.2mm
5) Downward movement
   T5=0.42s, H1=6.8mm
6) Beginning of the lower reverse movement
   T6=0.47s, H0=0mm

The measured signals have been used to calculate the moment during the process according to the formulas explained above. The signal of the cone force in Figure 7 is around 100N, the steps that can be seen are generated by the feeding movement of the honing stone. They occur every 0.25s which is exactly the value of the time between feed steps. The axial force changes with the oscillation movement. It becomes zero at the reverse stops and is highest during the continuous contact between honing stone and work piece. The axial force is positive during the downward movement and negative during the upward movement.
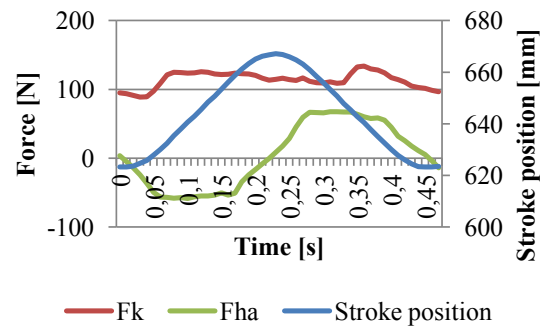
Fig. 7. Stroke position, cone force Fk and axial force Fha measured during the process (one oscillation).

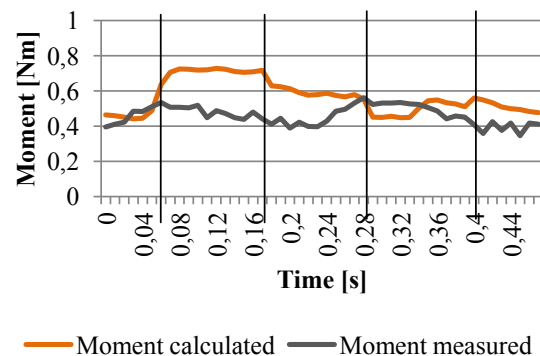## 5. Comparison between measured and calculated signal

Fig. 8. Comparison of measured and calculated signal.

Figure 8 shows the comparison between the calculated signal and the measured signal in the different phases. One can see that they fit rather well regarding phase 1, 4, 5 and phase 6. In phase 2 and 3, the deviations are significantly higher. Reasons for the deviations in the signal could be found in the measurement of the axial force. As the force sensor beneath the work piece takes the full axial force caused by the honing stone as well as the two guiding stones, there should be some error. For the calculation of the moment above, the signal of the axial force has been divided by three, as the force has been assumed the same at all three stones. Another error can stem from the assumption of the constant diameter of the bore for the calculation, which is not the case in reality.

6. Conclusion and Outlook

The paper shows a theoretical approach for a dynamic modeling of the honing process. A theoretical model has a high potential to improve the regulation of the honing process using a constant honing force. This would help to make honing fit for higher product variety and smaller lot sizes as it can help to reduce long running in periods for new processes. Another advantage is a better quality of the honed parts that could be reached through a constant process force. While the formulas here show a promising approach, there still remains a lot to do until the improved approach can be used for a new regulation. Further works should include the modeling of a whole honing process instead of only one oscillation as well as experiments using other workpiece materials and honing stones, e.g. honing stones with diamond grains working on untreated steel.

Acknowledgements

References

[1] Schmitt C, Bähre D, Forsch K, Klein H. Feinstbearbeiten hochgenauer Bohrungen durch Honen. Jahrbuch Schleifen, Honen, Läppen und Polieren, 65. Ausgabe; 2011. (only available in German, translated title: "Fine machining of precise bores through honing")

[2] Todd R, Allen D, Alting L. Honing. In: Manufacturing Processes Reference Guide: Industrial Press Inc; 1994. p. 65-70.

[3] Tolinski M. High-Performance Honing. Manufacturing Engineering, June 2008. Vol. 140, No.6.

[4] Bähre D, Schmitt C, Moos U. Comparison of Different Approaches to Force controlled Precision Honing of Bores. Proceedings of NAMRI/SME, Vol. 40; 2012.

[5] ElMaraghy H, Schuh G, ElMaraghy W, Piller F, Schönsleben P, Tseng M, Bernard A. Product variety management. CIRP Annals – Manufacturing Technology 62; 2013. p.629-652.

[6] Mushardt H. Modellbetrachtungen und Grundlagen zum Innenrundhonen. Ph.D. Thesis, TU Braunschwieg; 1986. (only available in German, translated title: "model analysis and basics for long-stroke honing")

[7] Zettel H-D. Abtragssteigerung und Formverbesserung beim Langhubhonen. Ph.D. Thesis, Universität Karlsruhe. 1974.(only available in German, translated title: "Increase of material removal and form improvement for long-stroke honing")

[8] Saljé E, von See M. Process-Optimization in Honing. Annals of the CIRP, Vol. 36/1; 1987.

[9] Schmitt C, Bähre D. An Approach to the Calculation of Process Forces during the Precision Honing of Small Bores. Proceedings of the 46th CIRP Conference on Manufacturing Systems, 2013.

[10]Hoffmeister, H.-W., Menze, B., 2004. Einsatz von Sensorik beim Honen und Regelung von Honprozessen. Jahrbuch Schleifen, Honen, Läppen und Polieren, 61. Ausgabe. (only available in German, translated title: "Use of sensors for honing and regulation honing processes")